Int J Thermophys (2012) 33:1814–1821
DOI 10.1007/s10765-012-1276-z

Non-invasive Glucose Measurements Using Wavelength Modulated Differential Photothermal Radiometry (WM-DPTR)

X. Guo · A. Mandelis · B. Zinman

Received: 9 February 2012 / Accepted: 7 August 2012 / Published online: 24 August 2012

Abstract Wavelength-modulated differential laser photothermal radiometry (WM-DPTR) is introduced for potential development of clinically viable non-invasive glucose biosensors. WM-DPTR features unprecedented glucose-specificity and sensitivity by combining laser excitation by two out-of-phase modulated beams at wavelengths near the peak and the baseline of a prominent and isolated mid-IR glucose absorption band. Measurements on water–glucose phantoms (0 to 300 mg/dl glucose concentration) demonstrate high sensitivity to meet wide clinical detection requirements ranging from hypoglycemia to hyperglycemia. The measurement results have been validated by simulations based on fully developed WM-DPTR theory. For sensitive and accurate glucose measurements, the key is the selection and tight control of the intensity ratio and the phase shift of the two laser beams.

Keywords Biosensor · Glucose · Middle infrared (MIR) · Wavelength-modulated differential laser photothermal radiometry (WM-DPTR)

1 Introduction

It is now well recognized that we are in the midst of a global epidemic of diabetes [1]. The disease is widely spread with more than 20 people being newly diagnosed

X. Guo (✉) · A. Mandelis
Department of Mechanical and Industrial Engineering, Center for Advanced Diffusion-Wave Technologies (CADIFT), University of Toronto,
5 King's College Road, Toronto, ON M5S 3G8, Canada
e-mail: guox@mie.utoronto.ca

B. Zinman
Mount Sinai Hospital, Samuel Lunenfeld Research Institute, University of Toronto,
60 Murray Street, Toronto, ON M5T 3L9, Canada

every hour of every day. Patients can be at serious risk depending on the concentration and duration of blood glucose values: low levels (hypoglycemia) for any length of time are associated with acute danger (brain damage, even death), while high levels (hyperglycemia) have a chronic impact over days or years which can damage organs, blood vessels, and nerves [2]. To prevent or delay complications, blood glucose monitoring is required [3]. However, the discomfort and pain of the current finger-pricking procedure lead to poor compliance. Over the past 20 years, researchers have been pursuing non-invasive methods of glucose monitoring. The most promising methods are optical technologies [4,5]. The spectral range of highest interest has been in the near-infrared (NIR) because of the relatively low water absorption [4,6]. However, the weak glucose absorption bands (overtone and combination bands) and confounding bands from other blood constituents make NIR methods impractical. In contrast, the middle-infrared (MIR) region has a prominent glucose absorption band which is peaked at ca. 9.7 μm, and is isolated from other interfering peaks in human blood [7–12]. Nevertheless, the MIR range has been less explored because of the overwhelming water absorption barrier.

We have developed a non-invasive technique, wavelength-modulated differential laser photothermal radiometry (WM-DPTR), experimentally and theoretically for continuous or intermittent glucose monitoring in the MIR range [13–15]. The WM- DPTR method consists of out-of-phase modulated laser-beam excitation at two discrete wavelengths near the peak (∼9.5 μm) and the baseline (∼10.4 μm) of the aforementioned glucose absorption band. Two quantum cascade lasers (QCL) are used, resulting in a differential blackbody emission detected via a HgCdZnTe (MCZT) detector (2 μm to 5 μm spectral detection bandwidth) as a photothermal up-conversion process. The differential method suppresses the strong background signal due to water absorption, while the narrow detector spectral bandwidth eliminates source–detector interference, thus greatly enhancing glucose detection sensitivity. Because of shallow penetration depth in the MIR range, WM-DPTR is designed to measure the glucose concentration in the interstitial fluid in the epidermis layer within 100 μm from the surface, which is correlated to a blood glucose concentration with ∼10 min delay. The measurement results from *intestinal fluid phantom*, aqueous glucose mixtures (0 to 300 mg/dl), demonstrate that both the amplitude and phase of the WM-DPTR signal can be used for glucose detection. The sensitivity and accuracy of glucose measurements rely on judicious selection and tight control of the intensity ratio and phase difference of the two laser beams.

2 Theory

The theoretical analysis of the WM-DPTR signal is based on differential photothermal radiometric signal generation following sequential optical absorption of two out-of-phase square-wave modulated laser beams by a semi-infinite one-dimensional medium [15]. The sensitive glucose detection stems from the selective absorption of the glucose molecule at two excitation wavelengths (peak and baseline of glucose absorption band). The differential signal arises because the absorption maximum (one laser beam) generates a photothermal-wave centroid for the IR emission closer to the surface than

the absorption minimum (the other laser beam). In addition, changes in the thermophysical properties of the water–analyte mixture compared to those of pure water act as a differential signal amplifier in WM-DPTR. The PTR signal generated by a single laser is as follows:

$$\begin{aligned} S_j(t) &= \Delta Q_j(t) \\ &= \left[\frac{\bar{\mu}_{\mathrm{IR}} K(\lambda_1,\lambda_2)\alpha}{2k}\right] I_{0j}\mu_{ej}\tau_{tj} \\ &\quad \times \left\{ \begin{array}{l} \frac{1}{\bar{\mu}_{\mathrm{IR}}+\mu_{ej}}\left[W\left(\sqrt{\frac{t}{\tau_{tj}}}\right)+W\left(\sqrt{\frac{t}{\tau_{\mathrm{IR}}}}\right)-2\right] \\ \quad +\frac{1}{\bar{\mu}_{\mathrm{IR}}-\mu_{ej}}\left[W\left(\sqrt{\frac{t}{\tau_{tj}}}\right)-W\left(\sqrt{\frac{t}{\tau_{\mathrm{IR}}}}\right)\right] \\ \quad +\frac{2}{\bar{\mu}_{\mathrm{IR}}}\left\{2\sqrt{\frac{t}{\pi\tau_{tj}}}-\sqrt{\frac{\tau_{\mathrm{IR}}}{\tau_{tj}}}\left[1-W\left(\sqrt{\frac{t}{\tau_{\mathrm{IR}}}}\right)\right]\right\} \end{array} \right\}; \quad j=A,B, \end{aligned} \tag{1}$$

where $\bar{\mu}_{\mathrm{IR}}$ is the spectrally weighted IR absorption/emission coefficient for homogeneous absorbers, $K(\lambda_1,\lambda_2)$ is a factor related to the detector collection bandwidth $[\lambda_1,\lambda_2]$, α and k are the thermal diffusivity and thermal conductivity of the medium, respectively, I_{0j} is the laser beam intensity, μ_{ej} is the optical absorption coefficient, $\tau_{tj} \equiv \frac{1}{\mu_{ej}^2\alpha}$ is a photothermal time constant indicating heat conduction in the photo-excited medium from a distance equal to the optical absorption depth, $W(x) \equiv \mathrm{e}^{x^2}\mathrm{erfc}(x)$, and $\tau_{\mathrm{IR}} \equiv \frac{1}{\alpha\bar{\mu}_{\mathrm{IR}}^2}$ is a photothermal time constant indicating conductive heat transfer from a length equal to the mean infrared optical absorption depth, $1/\bar{\mu}_{\mathrm{IR}}$.

Over the full square optical waveform repetition period $0 \le t \le \tau_0$, the sequence of photothermal responses is as follows:

$$S_{\mathrm{AB}}(t) = \left\{ \begin{array}{ll} \Delta Q_{\mathrm{A}}(t); & 0 \le t \le \frac{\tau_0}{2} \text{ (laser A on; laser B off)} \\ \Delta Q_{\mathrm{A}}(t) - \Delta Q_{\mathrm{A}}\left(t-\frac{\tau_0}{2}\right) + \Delta Q_{\mathrm{B}}\left(t-\frac{\tau_0}{2}\right); & \frac{\tau_0}{2} \le t \le \tau_0 \text{ (laser A off; laser B on)} \end{array} \right., \tag{2}$$

where $\tau_p = \tau_0/2$. For WM-DPTR with lock-in detection, the demodulated WM-DPTR signal at the fundamental angular frequency $\omega_0 = 2\pi/\tau_0$ is described by amplitude A and phase P:

$$\begin{aligned} A_{\mathrm{AB}} &= \sqrt{\Delta S_{\mathrm{IP}}^2 + \Delta S_{\mathrm{Q}}^2} \\ P_{\mathrm{AB}} &= \tan^{-1}\left(\frac{\Delta S_{\mathrm{Q}}}{\Delta S_{\mathrm{IP}}}\right), \end{aligned} \tag{3}$$

where $\Delta S_{\mathrm{IP}}(\omega_0) = \frac{2}{\pi}b_1(\omega_0)$ is in-phase and $\Delta S_{\mathrm{Q}}(\omega_0) = -\frac{2}{\pi}a_1(\omega_0)$ is quadrature with

$$\begin{bmatrix} a_1(\omega_0) \\ b_1(\omega_0) \end{bmatrix} = \frac{\omega_0}{\pi}\int_0^{\tau_0} S_{\mathrm{AB}}(t)\begin{bmatrix} \cos(\omega_0 t) \\ \sin(\omega_0 t) \end{bmatrix} \mathrm{d}t. \tag{4}$$

3 Materials and Method

Water–glucose mixtures were obtained by dissolving D-glucose in deionized water. Accurate glucose concentrations of the mixtures were determined using a biochemistry analyzer (YSI 2700S, Life Sciences, OH). The glucose detection range (0 to 300 mg/dl) was chosen to monitor both hyperglycemia and hypoglycemia, the two problematic ranges in diabetes blood–glucose regulation. An experimental WM-DPTR system was developed as shown in Fig. 1. The setup consisted of two QCLs and a laser controller (QCL, 1101-95/104-CW-100-AC, Pranalytica, CA) emitting at 9.5 μm and 10.4 μm, a HgCdZnTe detector (MCZT, PVI-4TE-5, Vigo System, Poland) sensitive in the 2 to 5 μm spectral bandwidth, a function generator (33220A, Agilent Technologies, CA) generating two phase-locked square waves to modulate the laser beams, and a lock-in amplifier (SR850, Stanford Research Systems, CA). When the two out-of-phase square-wave modulated laser beams irradiate the sample *on the same spot, optimized* differential PTR signals are generated. The signal is collected by the MCZT detector and then sent to the lock-in amplifier for demodulation. The laser intensity ratio is controlled by a motorized variable circular nuetral density filter (Reynard Corp, CA) in front of laser B, and the phase shift between two laser beams is controlled by the function generator.

4 Results and Discussion

WM-DPTR is sensitive to glucose. However, the sensitivity highly relies on two important parameters: amplitude ratio R and phase shift dP, defined as the ratio of pure water

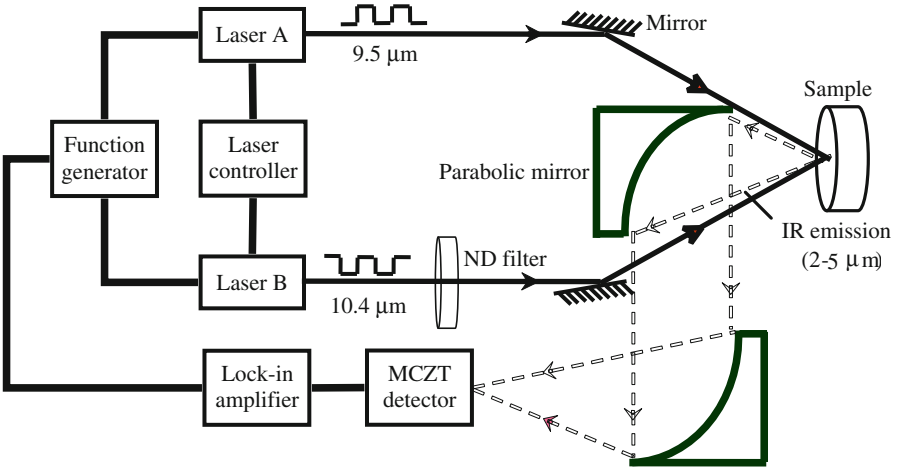

Fig. 1 Schematic diagram of WM-DPTR system. Square-wave modulated radiation from laser A (9.5 μm) and laser B (10.4 μm) co-incident on the sample generate superposed IR emissions. The differential infrared photon flux is collected by the MCZT detector acting as a bandpass filter (2 μm to 5 μm, *dashed line*) and sent to a lock-in amplifier. The function generator controls the phase shift between the two laser beams, and the variable circular neutral density (ND) filter controls the intensity ratio of the two lasers

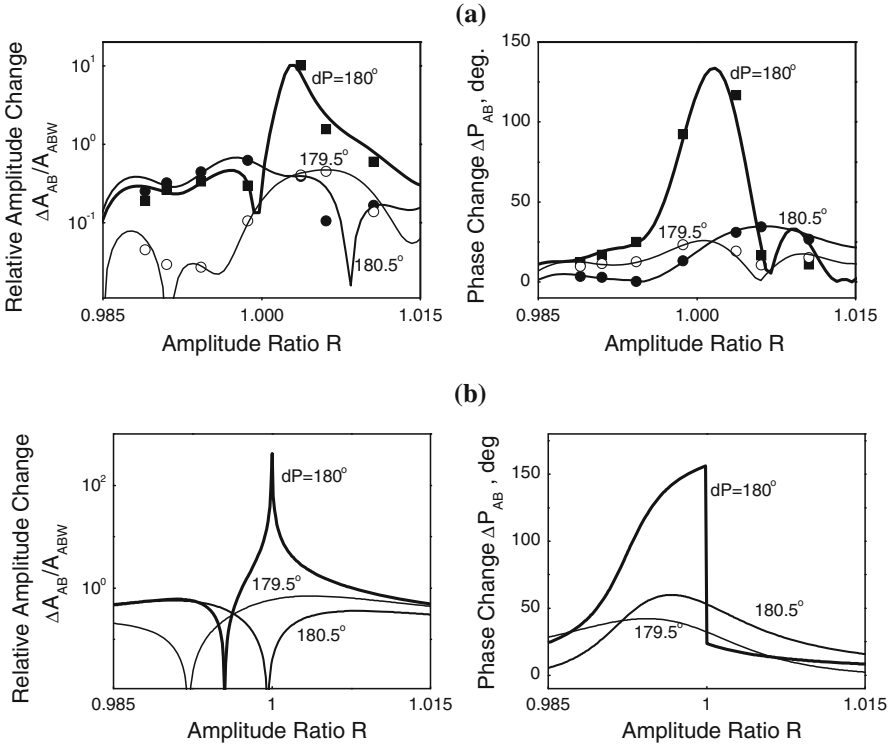

Fig. 2 Amplitude ratio R and phase shift dP dependence of WM-DPTR glucose sensitivity: differential signal change resulted from 0 to 300 mg/dl glucose concentration change: (a) experimental results; the points are raw measurement data and the *lines* are interpolated data and (b) theoretical simulation results

PTR amplitudes and phase differences generated from laser A and laser B alone: $R = A_{\mathrm{Aw}}/A_{\mathrm{Bw}}$, $\mathrm{d}P = P_{\mathrm{Aw}} - P_{\mathrm{Bw}}$. Thus, implementing tight R and dP controls is a very important part of the WM-DPTR system development. Amplitude ratio R tuning can be realized by fixing the beam intensity of one laser while changing that of the other laser, resulting in corresponding change in baseline signal amplitudes. To meet the high resolution and phase-independence requirements, the R control system has been upgraded from mechanical (through iris) to electrical (by tuning laser input voltage), and finally to the current optical control (tuning a variable neutral density filter). The phase shift of baseline signals is mainly determined by the phase shift between the two laser beams. The phase shift control was also upgraded from a preset fixed phase shift (∼180°) to current high-resolution tunable phase shift control through a phase-locked function generator. The following measurements were performed with the latest upgraded WM-DPTR system.

The R and dP dependence of WM-DPT glucose sensitivity is shown in Fig. 2. Figure 2a displays the measured WM-DPTR signal amplitude change, $\Delta A_{\mathrm{AB}}/A_{\mathrm{ABw}}$ ($\Delta A_{\mathrm{AB}} = A_{\mathrm{AB}} - A_{\mathrm{ABw}}$), between pure water ($A_{\mathrm{ABw}}$) and 300 mg/dl glucose solution (A_{AB}), and the respective phase change, $\Delta P_{\mathrm{AB}} = P_{\mathrm{AB}} - P_{\mathrm{ABw}}$, against amplitude ratio R. As indicated, WM-DPTR signals are most sensitive to glucose at $R \sim 1$

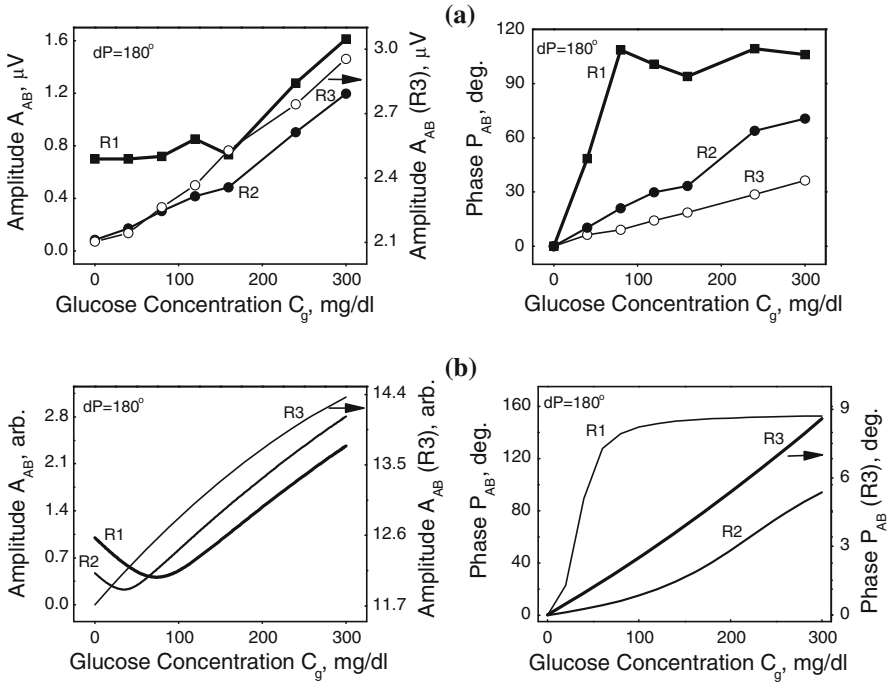

Fig. 3 Linearity of WM-DPTR signal response to glucose (0 to 300 mg/dl concentrations) with fixed phase shift d$P = 180°$ and varying amplitude ratio R from 0.97 to 1.03. (a) Experimental results and (b) simulation results

with phase shift d$P = 180°$, with ca. 10 times change in amplitude and ca. 140° change in phase. With a phase shift change (as small as 0.5°) away from 180°, the glucose sensitivity drops greatly, only ∼100 % change in amplitude and ∼40° change in phase. The measurement results were verified by simulation results based on Eq. 2, see Fig. 2b. Under ideal conditions, the simulation results exhibit even higher sensitivity. With detailed glucose concentration measurements, it was found that the WM-DPTR glucose sensitivity is not always linear in the clinically related glucose concentration range (0 to 300 mg/dl) as shown in Fig. 3. Figure 3a displays the WM-DPTR signals versus glucose concentration with ∼40 mg/dl glucose concentration intervals measured with fixed phase shift d$P = 180°$ and different amplitude ratio R, ranging from 0.97 to 1.03. It can be seen clearly that different R favor different potential applications: for the amplitude, $R1$ is suitable for hyperglycemia, $R2$ for hypoglycemia, and $R3$ for the full range. Even though the relative amplitude change with $R3$ is smaller, the higher amplitude level makes it more readily measureable with a higher SNR. For the phase, $R1$ is preferable for hypoglycemia, $R2$ for hyperglycemia, and $R3$ for the full range. The measurement results are well in agreement with the simulation results of Fig. 3b. The strong R dependence at d$P = 180°$ shown in Fig. 2 requires high-precision control of R which makes accurate measurements extremely difficult, even impossible. However, the R-dependence is lessened if the phase shift is slightly away from 180°, at the cost of some sensitivity to glucose. The achievement of the greatest

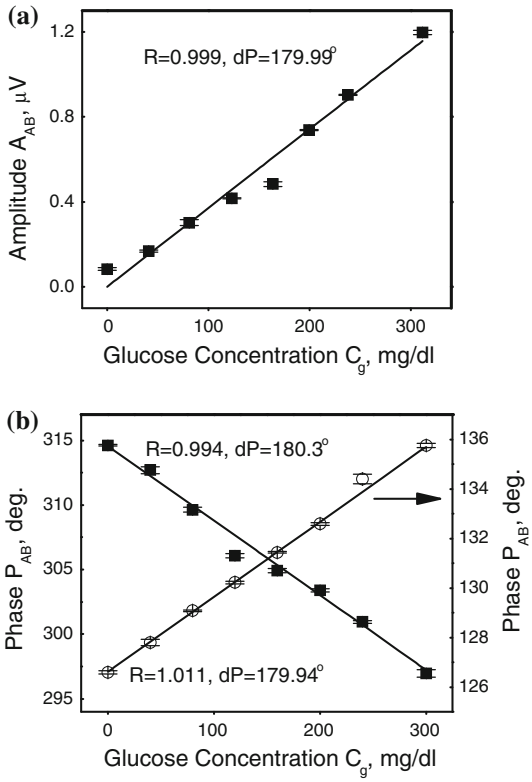

Fig. 4 Optimal $R-\mathrm{d}P$ combinations for linear WM-DPTR signal response to glucose. (a) Measured linear amplitude response and (b) measured linear phase response

glucose sensitivity and measurement accuracy depends on the optimal combination of R and dP. With the current WM-DPTR system and automated R–dP setting (ND filter and function generator) controlled by the computer, optimal R–dP combinations have been found for optimally sensitive glucose measurements with near-linear amplitude ($R^2 = 0.966$) and phase ($R^2 = 0.987$ and 0.995, respectively) responses, see Fig. 4. The error bars on the data points are the results of the standard deviation from five sequential measurements. The predictive errors in the above measurements are Fig. 4a: 12.9 mg/dl in the $C_g < 75$ mg/dl range and 19 mg/dl in the $C_g > 75$ mg/dl range; Fig. 4b: 8.1 mg/dl and 5 mg/dl in the $C_g < 75$ mg/dl range, 11/5 mg/dl and 7 mg/dl in the $C_g > 75$ mg/dl range. These variances are well below the accuracy criteria set by the International Organization for Standardization (15 mg/dl for $C_g < 75$ mg/dl and 20 % for $C_g > 75$ mg/dl). This is a significant achievement for this inherently nonlinear differential-signal methodology which should facilitate its penetration into clinical practice. It should be noticed that the amplitude curve shown in Fig. 4a is not under the same $R-\mathrm{d}P$ conditions as the phase curves in Fig. 4b. It turns out that either amplitude or phase (not both) can be linearized for a given optimized $R-\mathrm{d}P$ combination. At this juncture, we lean toward phase linearization at the expense of amplitude because the signal level is higher under the optimal $R-\mathrm{d}P$ condition of phase curves.

5 Conclusions

We have reported the development of a WM-DPTR system for potential application in non-invasive blood glucose measurements. It has been demonstrated that WM-DPTR has great sensitivity to glucose in the clinically relevant concentration range. The achievement of the greatest glucose sensitivity and measurement accuracy relies on the optimal combination of two parameters: amplitude ratio R and phase shift $\mathrm{d}P$ of the two single baseline (water) signals. The implementation of a motorized circular variable neutral density filter and phase-locked function generator into the system has resulted in high R resolution (0.003) and high $\mathrm{d}P$ resolution (0.05°). The optimal $R-\mathrm{d}P$ combinations have been found for linear and stable WM-DPTR response to glucose in the human blood–glucose concentration range. The theoretical analysis of the WM-DPTR response has generated a solid foundation for understanding the physics behind the WM-DPTR method and is serving as a guide for crucial experimental signal parameter optimizations.

Acknowledgments The support of the NSERC-CIHR CHRP program, the Ontario Ministry of Research and Innovation (MRI), and the Canada Foundation for Innovation (CFI) is gratefully acknowledged. We are grateful to Pranalytica, Inc. for helpful discussions on, and partial support of, the QCL system.

References

1. M. Jones, J.M. Harrison, Diabetes Technol. Ther. **4**, 351 (2002)
2. M.B. Davidson, *Diabetes mellitus—Diagnosis and Treatment*, 3rd edn. (Churchill Livingstone, New York, 1991), pp. 231–232
3. S. Auxter, Clin. Chem. News **5** (1996)
4. R. McNichols, G. Coté, J. Biomed. Opt. **5**, 5 (2000)
5. A. Tura, A. Maran, G. Pacini, Diabetes Res. Clin. Pract. **77**, 16 (2007)
6. V.V. Tuchin (ed.), *Handbook of Optical Sensing of Glucose in Biological Fluids and Tissues*, 1st edn. (CRC Press, Boca Raton, 2008)
7. C.J. Pouchert, *The Aldrich Library of Infrared Spectra*, 3rd edn. (Aldrich Chemical Co., Milwaukee, 1981)
8. H.A. MacKenzie, H.S. Ashton, S. Spiers, Y. Shen, S.S. Freeborn, J. Hannigan, J. Lindberg, P. Rare, Clin. Chem. **45**, 1587 (1999)
9. G.B. Christison, H.A. McKenzie, Med. Biol. Eng. Comput. **31**, 284 (1993)
10. W. Martin, S. Mirov, R. Venugopalan, Appl. Spec. **59**, 881 (2005)
11. W. Martin, S. Mirov, R. Venugopalan, J. Biomed. Opt. **7**, 613 (2002)
12. P. Zheng, C.E. Cramer, C.W. Barnes, J.R. Braig, B.B. Sterling, Diabetes Technol. Ther. **2**, 1 (2000)
13. A. Mandelis, X. Guo, US Patent pending No. 12/948,525 (2010)
14. X. Guo, A Mandelis, A. Matvienko, K. Sivagurunathan, B. Zinman, J. Phys. Conf. Ser. **214**, 012025 (2010)
15. A. Mandelis, X. Guo, Phys. Rev. E **84**, 041917 (2011)